RSC Advances

ROYAL SOCIETY OF CHEMISTRY

www.rsc.org/advances

Journal Name

ARTICLE

N-Terminal Aromatic Tag Induced Self Assembly of Tryptophan-Arginine Rich Ultra Short Sequences and Their Potent Antibacterial Activity

Received 00th January 20xx,
Accepted 00th January 20xx

DOI: 10.1039/x0xx00000x

www.rsc.org/

Seema Joshi,[a, b] Rikeshwer P. Dewangan,[a, c] Mohammad Shahar Yar[c], Diwan S. Rawat[d] and Santosh Pasha[a, *]

Multiple drug resistant (MDR) *Staphylococcus aureus* is among the most dreaded pathogens for human health in community as well as nosocomial environments. Here we report self assembling ultra short N-terminal modified peptidomimetics based on a template X-W_3R_4 (where, X = aromatic organic moiety) that show potent activity against multiple MDR *S. aureus* strains. The active sequences self assemble in water to form nano vesicle (140-190 nm diameter) with positive surface zeta potential and hydrophobic core of Trp residues/N-terminal tags. Further, lethal membrane depolarisation of MRSA cells and a concentration dependent leakage of calcein dye from artificial bacterial mimic membranes established membrane disruptive mode of action for designed sequences. We demonstarte role of N-terminal tag on nature of self assembly and envisage the origin of antibacterial activity to be conformationally aligned nanovesicles which upon interaction lead to disruption of bacterial cells. The designed cell selective nanovesicles may further be exploited towards in vivo applications as antibacterial agent alone or as vehicles for systemic anti-infective therapy.

1. Introduction

Infectious diseases caused by MDR pathogens are rendering antibiotic therapy more difficult and costly at an unprecedented rate [1]. According to a recent report by World Health Organization (WHO) the global antimicrobial drug resistance has reached at an alarming stage where in very near future even common infections and minor injuries might lead to mortality due to inefficacy of antibiotics to cure [2]. The development of resistance is aggravated by irrational use of antibiotics in livestock and medical practices that has armed microbes with multitude of novel drug resistance mechanisms. In the present scenario, no class of antibiotics with a fixed metabolic target in microbes are free from the resistance development problem. Therefore, currently a pressing need is being felt to discover novel antibiotics from yet under explored sources and impede the prevalent practices that are leading towards MDR bacterial strains [3, 4].

To address this concern host defence cationic peptides (HDCPs) are good alternative as they are part of evolutionary conserved innate immunity [5]. Unlike conventional antibiotics that target five fundamental macromolecular synthesis pathways, HDCPs act by multitude of novel mechanism of action primarily impairing membrane architecture [6]. With amphipathic patterns (segregation of cationic and hydrophobic residues) HDCPs present prototypical examples of structure based active molecules, where secondary structure acquired in the vicinity of bacterial membranes play a crucial role in activity and cell selectivity [7]. For membrane active peptides, the secondary structure mediated folding and self association leads to transient pore formation that comprise of bunch of peptides clustered together which may acquire defined nanostructures/aggregates [8]. Such peptide or peptide/lipid aggregates may also lead to clustering of lipids causing defects in membrane architecture that ultimately leads to membrane damage/release of intra cellular contents ensuing cell death [9, 10]. Further, the existence of HDCPs mediated pores that are not only

[a]*CSIR- Institute of Genomics and Integrative Biology, Mall Road, Delhi, India. Fax: +91 1127667471; Tel: (91) (011) 27666156; E-mail: spasha@igib.res.in*
[b]*Current affiliation: School of Environmental Sciences, Jawaharlal Nehru University, Delhi, India*
[c]*Department of Pharmaceutical Chemistry, Faculty of Pharmacy, Jamia Hamdard, New Delhi, India*
[d]Department of Chemistry, *University of Delhi, Delhi, India*
Electronic Supplementary Information (ESI) available: HPLC chromatogram, ESI-MS spectra, size and zeta potential histograms along with CAC plots
DOI: 10.1039/x0xx00000x

transient but persist and expand causing irreversible closing has now been established for some of the peptides [11].

However, the untoward side effects associated with HDCPs are high production costs, associated toxicity and low serum stability [12]. Therefore over the past decades remarkable efforts have been put to design novel short HDCPs mimics, some of which are under clinical trials at present [13, 14]. More recently, supra-molecular assemblies with peptide amphiphiles or organic polymers are capturing attention for design of HDCPs mimics [15-17]. Several reports have established a positive correlation between the propensity for self assembly of the peptide/polymer on their penetration power and bactericidal activity [18, 19].

Several HDCPs e.g. tritrypticin, indolicidin, defensins and cathelicidins contains numerous Arg and Trp residues [20]. A number of novel sequences based on Trp and Arg residues have also been reported with potent antibacterial activity [21-23]. Keeping this in mind and based on our previous work on design of novel N-terminal modified peptidomimetics [24-26]; in the present work, we explored self assembling N-terminal aromatic tag based ultra short Trp and Arg rich sequences as potent, biodegradable antibiotic candidates to combat clinically relevant drug resistant Gram-positive bacterial strains. Further we deciphered mode of action of active sequences on artificial membranes and bacterial cells to dissect the importance of self assembly and organization on antimicrobial activity and mode of action.

2. Experimental

2.1 Chemicals

Fluorenylmethoxycarbonyl (Fmoc)-protected amino acids and resins were purchased from Novabiochem (Darmstadt, Germany). N-terminal aromatic tagging, piperidine, N-hydroxybenzotrizole (HOBt), 1,1,1-trifluoroethanol (TFE), trifluoroacetic acid (TFA), N,N-diisopropylcarbodiimide (DIPCDI), triisopropylsilane (TIS), calcein and 3,3′-dipropylthiadicarbocyanine iodide ($DiSC_3(5)$), Dulbecco's modified Eagles' Medium (DMEM), heat inactivated fetal bovine serum (FBS), trypsin from porcine pancreas and 3-(4,5-dimethyl-2-thiazolyl)-2,5-diphenyl-2H tetrazolium bromide (MTT) were obtained from Sigma Chemical Co. (St Louis, MO, USA). 1,2-Dioleoyl-sn-glycero-3-phosphocholine (DOPC) and 1-palmitoyl-2-oleoyl-sn-glycero-3- phospho-(1'-rac-glycerol) (sodium salt) (DOPG) were purchased from Avanti Polar Lipids. All solvents used for the purification were of HPLC grade and obtained from Merck (Darmstadt, Germany). Dimethylformamide (DMF) and dichloromethane were obtained from Merck (Mumbai, India). DMF was double-distilled before use.

2.2 Synthesis and purification of designed sequences

Fmoc based solid phase peptide synthesis strategy was used for synthesis of designed sequences on Rink amide MBHA resin [27]. All the coupling reactions were effectuated using 4 equivalents of DIPCDI and HOBt with 4 equivalents of the amino acid or N-terminal tagging. For deprotection 20% piperidine in DMF was used. Coupling and deprotection was detected based on Kaiser Test. Purification of all the sequences was done on semi preparative RPHPLC column (C18, 7.8 mm x 300 mm) with linear gradients of water containing 0.1% TFA (gradient A) and acetonitrile containing 0.1% TFA (gradient B) at a flow rate of 2.0 ml/min with 10-90% gradient B/min, starting at a concentration of 10% gradient B. The correct sequences after purification were characterized by LC-ESI-MS (Quattro Micro API Waters, USA).

2.3 Size and Zeta potential

The purified sequences were dispersed in water at 1 mg/mL and diluted up to 0.1 mg/mL in water. After filtration through a 0.45 μM filter the hydrodynamic radius/zeta potential was measured through dynamic light scattering (DLS). The DLS instrumentation consisted of a Malvern Zetasizer NanoS instrument, operating at 25 °C with a 4 mW He-Ne 633-nm laser module. Measurements were made at a detection angle of 173° (back scattering). DLS measurements were taken after equilibrating the samples for 2 min at 25 °C by recording measurements in triplicate (with 15 runs recorded per measurement).

2.4 High resolution transmission electron microscopy (HR-TEM)

The morphologies of nano assemblies formed by the designed sequences were observed under a FEI Tecnai G^2 electron microscope using an acceleration voltage of 120 keV. The samples were prepared by dissolving samples at 1 mg/mL in MQ water and subsequent dilution to 0.1 mg/mL. After filtration through 0.45 μM syringe filter a drop of aqueous sample was placed over a coated 200 mesh copper grid. After 1 min, the excess solution was blotted using filter paper. Then a 2% w/v solution of phosphotungstaic acid was used as a staining agent for 30 sec. The grids were dried and then visualized under electron microscope.

2.5 Critical aggregation concentration (CAC)

For designed sequences CAC values were determined using static light scattering (SLS) measurements on a spectrofluorometer (Jobin Yvon, FluoroMax-4; Horiba Scientific, Edison, NJ, USA) as described previously [28]. Briefly, the lyophilized sequences were dispersed at 1 mg/mL in MQ water at room temperature. The sample was diluted 2 fold in Mueller-Hinton broth Media (growth medium used for MIC determination). Further, serial ten-fold dilutions of the sequences were prepared in the same medium to get concentrations in the range of (0.05-500 μg/mL). The samples were subjected to light scattering using 90° geometry to collect the scattering intensity at 402 nm upon excitation of sample at 400 nm. Slit widths for both excitation and emission were fixed at 2.5 nm. For determination of CAC, intensities of scattered signal were plotted against peptidomimetic concentration. CAC was determined from the inflection point which was defined as the abscissa where the intensity rises steeply.

2.6 Circular dichroism

The Circular Dichroism (CD) spectra of sequences were recorded on a Jasco J-815 CD spectrophotometer (Tokyo, Japan) with a 1 cm path length cell. Wavelengths from 190 to 260 nm were scanned with 1.0 nm step resolution, 100 nm/min speed, 0.4 second response time, and 1 nm bandwidth. CD spectra were collected and averaged over three scans in MQ water, 5 mM sodium phosphate buffer (pH 7.2), and helix inducing solvent TFE (50% (v/v)). Spectra were baseline corrected by subtracting a blank spectrum containing only MQ, buffer or TFE (50% v/v). The spectrum was acquired at a sample concentration of 20 μg/mL. The experiment was repeated on two different days and reproducible results were obtained. Representative data expressed as ellipticity [θ] vs. wavelength as was obtained from the instrument is presented here.

2.7 Tryptophan fluorescence

To locate the position of tryptophan residues in nanovesicles we measured Trp fluorescence in water, buffer, artificial membranes and dimethyl sulphoxide (DMSO). Small unilamellar vesicles were used as artificial membrane. The procedure used for the preparation of SUVs was similar to that described previously [29, 30]. For bacterial mimic membranes a mixture of (DOPC: DOPG, 7:3, w/w) was used and as mammalian mimic systems DOPC SUVs were employed. For the Trp fluorescence experiment, each sequence (final concentration 5 μg/ml) was added to 500 μL of MQ, 10 mM Tris buffer (0.1 mM EDTA, 150 mM NaCl, pH 7.4), 10 mM Tris buffer containing 500 μg/ml SUVs or pure DMSO. Fluorescence measurements were performed in a quartz cuvette with a 1-cm path length on a spectrofluorometer (Jobin Yvon, FluoroMax-4; Horiba Scientific, Edison, NJ, USA). Samples were excited at 280 nm and emission was scanned from 300 to 450 nm at 1-nm increments. The excitation and emission slits were fixed at 5 nm. Spectra were corrected by blank subtraction for each medium. The experiment was repeated on three different days and was found to be reproducible. Representative emission spectra are presented here.

2.8 Antibacterial activity

Antibacterial activity was evaluated using serial broth dilution method as reported previously [30, 31]. Bacterial strains used were as follows, *E. coli* (ATCC 11775), *P. aeruginosa* (ATCC 25668), *S. aureus* (ATCC 29213), *E. faecalis* (ATCC 7080), *S. aureus* (ATCC BAA-44), *B. subtilis* (ATCC 6633), methicillin resistant *S. aureus* (ATCC 33591), *S. epidermidis* (ATCC 12228), and MRSE (ATCC 51625). The inoculums were prepared from mid-log phase bacterial cultures. Each well of the first 11 columns of a 96-well polypropylene micro titre plate (SIGMA) was inoculated with 100 μL of approximately 10^5 CFU/mL of bacterial suspension in Mueller-Hinton broth (MHB, DIFCO). Then 11 μL of serially diluted test sequences in 0.001% acetic acid and 0.2% bovine serum albumin (SIGMA) over the desired concentration range was added to the wells of micro titre plates. The micro titre plates were incubated overnight with agitation (200 rpm) at 37 °C. After 18 h absorbance was read at 630 nm. Cultures (approximately 10^5 CFU/mL) without test sequences were used as a positive control. Un-inoculated MHB was used as a negative control. Tests were carried out in duplicate on three different days. Minimum inhibitory concentration (MIC) is defined as the lowest concentration of test sequences that completely inhibits growth.

2.9 Bactericidal Kinetics

The kinetics of bacterial killing by sequences against MRSA (ATCC 33591) was determined at concentrations corresponding to 2 × and 4 × MIC. Briefly, log-phase bacteria ~1.3×10^6 CFU/mL in fresh MHB were incubated with desired sequences at 2 × MIC or 4 × MIC in MHB at 37 ºC. At fixed time intervals (0, 1, 2, 4, and 6 h) aliquots were removed and diluted in sterile saline before plating on Mueller-Hinton II agar plates. The plates were incubated at 37°C for 24h and CFU were counted. The experiment was performed in duplicates on three different days, and curves were plotted for $\log_{10}$CFU/ml versus time.

2. 10 Hemolytic activity and cytotoxicity

Hemolytic activity of the sequences was determined on human red blood cells (hRBC) as described previously [30, 32]. Briefly, 100 µL of desired concentration of sequences (two-fold serial diluted in PBS (35 mM sodium phosphate, 150 mM NaCl, pH 7.2)) was plated into sterilized 96-well plates and then a 100 µL suspension of hRBCs in buffer 4% v/v was added to each well. The plates were incubated for 1 h at 37 °C without agitation and centrifuged at 1500 rpm for 5 min. Aliquots (100 µL) of the supernatant were transferred to 96-well plates, where hemoglobin release was monitored using ELISA plate reader (Molecular devices) by measuring the absorbance at 414 nm. Percent hemolysis was calculated by the following formula:

$$\text{Percentage hemolysis} = 100(A-A_0)/(A_t-A_0)$$

where, A represents absorbance of peptide sample at 414 nm and A_0 and A_t represent zero percent and 100% hemolysis determined in PBS and 1% Triton X-100, respectively.

To assess cell viability, MTT assay was performed on A549 cell line as described previously [33]. Briefly, 5000 cells per well, were seeded in 96-well plates in DMEM low glucose media supplemented with 10% FBS to grow overnight. The next day media was aspirated and fresh media was added (50 µL per well). To the wells serial two-fold dilutions of different test samples (50 µL) were added and the plates were incubated at 37 °C with 5% CO_2 for 18 h. After 18 h the media was aspirated and 100 µL of MTT solution was added to each well. The plates were further incubated for 4 h in CO_2 atmosphere at 37 °C. After 4 h the MTT-containing medium was removed by aspiration. The blue formazan product generated was dissolved by the addition of 100 µL of 100% DMSO per well. The plates were then gently swirled for 2-3 min at room temperature to dissolve the precipitate. The absorbance was monitored at 540 nm. Percentage viability was calculated based on the formula:

$$\%\ \text{cell viability} = A/A_{con} * 100$$

Where, A represents sample absorbance at a given concentration and A_{con} represents absorbance for untreated cells.

2.11 Calcein leakage

The ability of designed sequences to cause leakage from artificial LUVs composed of bacterial mimic membrane (DOPC/DOPG) was accessed using a protocol as described previously [24]. Briefly, desired mixtures of the lipids DOPC/DOPG (7: 3, w/w) were dissolved in a 2 mL chloroform-methanol mixture in a 100 mL round bottom flask. The solvent was removed under a stream of nitrogen and the lipid film obtained was lyophilized overnight to remove any traces of organic solvent. The dry lipid films were rehydrated with 10 mM Tris-HCl [70 mM calcein, 150 mM NaCl, 0.1 mM EDTA]. The liposome suspension obtained after rehydration was freeze thawed for five cycles and extruded 16 times through two stacked polycarbonate filters (Mini extruder, Avanti Polar Lipids). Free calcein was removed by passing the liposome suspension through a Sephadex G-50 column at 23 °C and eluting with a buffer containing 10 mM Tris-HCl [150 mM NaCl, 0.1 mM EDTA]. After passing the liposome through a Sephadex G-50, liposome diameter was measured by dynamic light scattering using a Zetasizer Nano ZS (Malvern Instruments). The average diameter of LUVs was found to be in the range of 70-100 nm. Different concentrations of test sequences were incubated with DOPC/DOPG LUVs for 5 min before exciting the samples. Leakage was monitored by measuring the fluorescence intensity at an emission wavelength of 520 nm upon excitation at 490 nm on a model Fluorolog (Jobin Yuvon, Horiba) spectrofluorimeter. A slit width of 3 nm was used for both excitation and emission. Percentage dye leakage was calculated using the formula

$$\%\ \text{dye leakage} = 100 * (F- F_0/F_t-F_0)$$

Where, F is the fluorescence intensity achieved by addition of different concentrations of sequences. F_0 and F_t are fluorescence intensities in buffer and with Triton X-100 (20 µL of 10% solution) respectively. All measurements were made in duplicate and less than 7% deviation was obtained in the data points.

2.12 Membrane depolarization

For the evaluation of membrane depolarization a previously defined method was used [24, 34]. Briefly, overnight grown MRSA was sub cultured into MHB to obtain log phase cultures. The cells were centrifuged, washed, and re-suspended in respiration buffer (5 mM HEPES, 20 mM glucose, pH 7.4) to obtain a diluted suspension of OD_{600}~0.05. A membrane potential-sensitive dye, 3,3′-dipropylthiadicarbocyanine iodide ($DiSC_3$5), 0.18 µM (prepared in DMSO) was added to a 500 µL aliquot of the re-suspended cells and allowed to stabilize for 1 h. Baseline fluorescence was acquired using a Fluorolog (Jobin Yuvon, Horiba) spectrofluorometer by excitation at 622 nm and emission at 670 nm. Slit width of 5 nm was employed for excitation and emission. Subsequently, increasing concentrations of test sequences between 2.5 and 12.5 µg/mL were added to the cells and the increase of fluorescence on account of the dequenching of $DiSC_3$(5) dye was measured. Percent depolarization was calculated by using the formula

$$\%\ \text{depolarization} = (F- F_0)/(F_m- F_0)*100$$

Where, F is the fluorescence intensity 2 min after addition of sequences, F_0 is the initial basal fluorescence intensity, and F_m is the

maximum fluorescence intensity obtained after addition of 10 μg mL^{-1} gramicidin. The data was acquired on two different days and less than 4% deviation was observed in results. Percentage depolarization versus increasing concentrations is plotted here for different sequences.

2.13 Scanning electron microscopy

For electron microscopy freshly inoculated methicillin resistant *S. aureus* (ATCC 33591) was grown in MHB up to an OD_{600} of 0.5 (corresponding to 10^8 CFU/mL). Bacterial cells were then spun down at 4000 rpm for 15 min, washed thrice in PBS (20 mM, 150 mM NaCl) and re-suspended in an equal volume of PBS. The cultures were then incubated with test sequences at 10 × MIC (MIC concentration defined against 10^5 CFU/mL culture) for 30 min. Controls were run in the absence of sequences. After 30 min, the cells were spun down and washed with PBS thrice. For cell fixation the washed bacterial pallet was re-suspended in 1 mL of 2.5% glutaraldehyde in PBS and was incubated at 4 °C for 4 h. After fixation, cells were spun down and washed with PBS twice. Further the samples were dehydrated in series of graded ethanol solutions (30% to 100%), and finally dried in desiccators under vacuum. An automatic sputter coater (Polaron OM-SC7640) was used for coating the specimens with 20 nm gold particles. Then samples were viewed via a scanning electron microscope (EVO 40, Carl Zeiss, Germany).

3. Results and discussion

Design and synthesis of sequences

Sequence template approach is among of the most successful ways to design ultra short antimicrobial peptidomimetics based on balance between cationic (+2 to +9 charge) and hydrophobic residues (approximately 50%) [35, 36]. Most prevalent cationic residues present in HDCPs are Lys and Arg while Ile, Leu, Phe and Trp serve as the common hydrophobic residues. The cationic side chain of Arg with delocalized electron density provides an effective means of attracting the negatively charged bacterial cell surface through electrostatic and H-bonding interactions that facilitates binding with cell wall components such as lipopolysaccharides, teichoic acid or phospholipid head groups. Among common hydrophobic residues, Trp residues impart hydrophobicity along with a distinct ability to reside at membrane inter-phase improving antibacterial activity [20]. Therefore to design simple template based amphiphiles in the present work we exploited a Trp, Arg rich template with general formula X-W_3R_4 (where, X=aromatic hydrophobic tag) (Fig. 1). Initially to keep a minimum +4 charge we kept the number of Arg residues fixed (i. e 4) and varied the length of hydrophobic part by increasing number of Trp residues to enhance hydrophobicity. After attaching three Trp residues we achieved ~50% hydrophobicity (based on % of acetonitrile at RP-HPLC elution). Further, we incorporated aromatic N-terminal tags to significantly enhance hydrophobicity of sequence W_3R_4. As expected after attachment of N-terminal tag the overall hydrophobicity was increased and the sequences now comprised of 50% hydrophobic and 50% hydrophilic residues. Specifically 2-Fluoro-3-(trifluoro methyl) benzoic acid (in sequence 5), p-Terphenyl carboxylic acid (in sequence 6), and 2-methyl-1-naphthoic acid (in sequence 7) were used as N-terminal tags as these have been shown to enhance antibacterial activity while maintaining cell selectivity. Fluorine containing amino acids and small organic moieties have been shown to exhibit improved activity and better hydrophobic interactions with bacterial cells thereby improving the rate of bacterial cell penetration [37]. p-Terphenyl based α-helical mimics, presence of modified p-terphenyl moiety in FDA approved drug Anidulafungin along with several literature reports including our previous work established it to be a valuable antibacterial scaffold [25, 38]. Also, along with being a useful hydrophobic tag in various antibacterial peptidomimetics naphthoic acid containing molecules are components of small molecule efflux pump inhibitors in Gram-negative bacteria [39]. Therefore these aromatic tags were employed.

Fig. 1: Structural representation of designed template and different N-terminal tags. The hydrophilic residues are coloured blue and hydrophobic residues are coloured red.

The designed sequences were synthesized on Rink amine MBHA resin using standard solid phase Fmoc Chemistry. After cleavage from solid support, the crude peptide sequences were purified on C18 column using RP-HPLC and were characterized using LC-ESI-MS (Representative HPLC chromatogram and MS plots are shown in ESI). The designation, composition and % hydrophobicity of designed sequences are given in Table 1.

Characterization and biophysics of nanovesicles

The purified sequences were evaluated for their tendency towards nano-structuring in water (MQ). The driving force for self assembly of amphiphiles in water has been reported to be hydrophobic interactions among monomers. Here also we could see a N-terminal aromatic tag (hydrophobicity) driven assembly, as sequences 1-4 were devoid of nano structuring (hydrophobicity based on RP-

HPLC, 11.2-50.3%) whereas sequences 5-7 spontaneously formed ordered nano vesicles (hydrophobicity based on RP-HPLC, 62.8-74.5%). Using dynamic light scattering the diameter of nanovesicles formed by sequences 5-7 was found to be in the range of 142-190 nm. A stable positive zeta potential (40.7-47.9 mV) was also observed for the sequences 5-7 (Table 1) (Representative size distribution and zeta potential plots are shown in ESI Fig. 1 and ESI Fig. 2 respectively). Further, morphology of nanovesicles formed by sequences 5-7 were visualized under high resolution-TEM.

Fig. 2: Transmission electron microscopic images of sequences 5-7 in water.

Spherical empty vesicles with defined boundaries having diameter in the range of 100-120 nm were observed for sequence 5, 130-160 nm for sequence 6, and 90-180 nm for sequence 7 (Fig. 2). Topography of nanovesicles formed by sequences 5-7 were also confirmed by atomic force microscopy (AFM) and in accordance with TEM results spherical morphology was observed. Interestingly, in AFM data nanovesicles formed by sequence 5-7 also showed z-axis with height thus indicating presence of vesicles rather than micelles (data not shown here). Of note, under the influence of N-terminal aromatic tag sequences 5 and 6 with hydrophobicity >64% (as measured using RP-HPLC) formed smaller vesicles with narrow band widths and PDI whereas sequence 7 showed a broad width in diameter and relatively higher PDI.

We next evaluated critical aggregation concentration (CAC) of sequences 5-7 in Mueller Hinton Broth media (we chose MHB to correlate in vitro activity with self assembling concentration). For CAC determination light scattering intensity at 402 nm was recorded upon excitation of samples at 400 nm. The plot of concentration against relative change in fluorescence intensity revealed CAC to be 0.2 µg/mL for sequence 5, 3.0 µg/mL for sequence 6 and 3.9 µg/mL for sequence 7 (Table 1 and ESI Fig. 3). The low micro molar range CAC (<10 µg/mL) indicated facile self associating potential of designed sequences comparable to some of the active peptide amphiphiles [28].

We further characterized the nature of nanovesicles formed by these sequences making use of biophysical tools. We first acquired CD spectra of designed sequences in different milieus (water, phosphate buffer and 50% TFE (v/v)). The designed sequences are short therefore we deduce the CD spectra might largely be originating from the contribution of aromatic side chains in Trp residues rather than a secondary structure. Sequence 4 did not exhibit any spectral features in water, however, 5 mM phosphate buffer and 50% TFE (v/v) induced minima at 222 nm and 201 nm. Fascinatingly, sequences 5 and 7 exhibited the characteristic minima around 220-228 nm and 196-201 nm and maxima around 211-215 with pronounced increase in ellipticity in all three milieus (Fig. 3). Sequence 6 also showed similar spectral features however slightly diminished ellipticity was observed in buffer and 50% TFE as compared to water. De-convolution of CD data in all tested milieu lead to prediction of turn structure (20-40%) with almost 60-80% random coil conformation. The negative minima in the range of 220-230 nm coupled with the corresponding positive peak at 211-215 nm may here be attributed to exciton coupling between closely packed Trp residues as has been reported previously for multiple Trp containing peptides [40]. Overall, the observed ellipticity values pointed towards a turn conformation with combination of Trp stacking interactions implicating folding facilitated burial of aromatic N-terminal tagging and Trp residues inside the core of nanovesicles whereas hydrophilic, Arg residues occupied outer surface of the vesicles that resulted into a stable positive surface zeta potential for the designed sequences (ESI Fig. 2).

Fig. 3: CD spectra of designed sequences in different environments; water (◆), phosphate buffer (▪) and 50% TFE (v/v) (▲). In (a) Sequence 4, (b) sequence 5, (c) sequence 6 and (d) sequence 7. The spectrum was acquired at a sample concentration of 20 µg/mL.

We further evaluated the environment of Trp residues in the nanovesicles by measuring Trp fluorescence spectra of sequences 5-7 in various milieus (water, buffer, artificial lipids and DMSO). As a control we measured Trp fluorescence spectrum of sequence 4 as well. In sequence 4, the Trp residues were found to be freely fluorescing in water and buffer with emission maxima at 365 nm. Further, in artificial zwitterionic (DOPC) and mixed lipids (DOPC/DOPG, 7:3, w/w) a shift in environment of Trp residues was evident in sequence 4 as enhancement in fluorescence intensity and a concomitant blue shift (7 nm in zwitterionic and 13 nm in mixed SUVs) was observed (Fig. 4). At same tested concentration for sequences 5 and 6 great reductions in Trp fluorescence emission intensity were observed in water and buffer as compared to sequence 4. Due to presence of p-terphenyl tagging, the emission maxima in sequence 6 was shifted to ~405 nm in water as well as buffer as has been reported previously [25]. Interestingly, even in hydrophobic environments of artificial zwitterionic or anionic membranes, the Trp residues of sequence 5 and 6 were found to be buried (negative or baseline fluorescence) and thus not available to fluoresce. Only in

presence of organic solvent DMSO, sequences 5 and 6 showed slight increase in fluorescence intensity. Compared to sequences 5 and 6, sequence 7 showed some increase in Trp fluorescence intensity in all tested medium, although not as much as was observed for sequence 4. Recently, Trp fluorescence emission spectrum of a self associating thrombin derived peptide was shown to exhibit a blue shift in aqueous solvents on account of self association ability of the peptide [41]. The authors implicated partial exposure of the Trp residues to the aqueous environment responsible for this observed blue shift. Here, although we do not see a shift in emission maxima in aqueous environments we observed severe reduction in emission intensity that may be attributed to burial of Trp residues in sequence 5 and 6 inside the nano-vesicle core.

Fig. 4: Trptophan fluorescence spectra of designed sequences in different environments; water (◆), 10 mM Tris buffer (▬) DOPC (▲) DOPC/DOPG (■) and DMSO (■). In (a) Sequence 4, (b) sequence 5, (c) sequence 6 and (d) sequence 7. The spectrum was acquired at a sample concentration of 5 µg/mL.

Biological activity

We further evaluated designed sequences as antibacterial agents against a panel of Gram-positive and representative Gram-negative bacterial strains using serial broth dilution method. Sequences 1-4 were found to be inactive with minimum inhibitory concentrations (MIC) >45.4 µg/mL against all the tested strains, except sequence 4 which showed activity against S. *aureus* with MIC at 45.5 µg/mL. Further, increase in hydrophobicity lead to drastic improvement in potency of designed sequences 5-7 implicating role of increased hydrophobicity which in turn enhanced nano structuring and antibacterial activity (Table 2). We also evaluated antibacterial activity of N-terminal tagging molecules to know the contribution of tagging on activity. The results showed no growth inhibition with MIC> 100 µg/ml for all three N-terminal tags used here. The results showed that sequences with threshold hydrophobicity above 50% (calculated based on RP-HPLC retention time) showed potent activity against the bacterial strains tested. Sequences 5-7 caused potent growth inhibition against susceptible as well as clinically relevant pathogens including *S. aureus* (MIC: 1.4-2.8 µg/mL), *E. faecalis* (5.6-11.3 µg/mL), *S. epidermidis* (MIC: 0.7-1.4 µg/mL), ciprofloxacin resistant *S. aureus* (MIC: 1.4-2.8 µg/mL), MRSE (MIC: 0.7-1.4 µg/mL) and MRSA (MIC: 1.4-2.8 µg/mL).

Against representative Gram-negative bacterial strains *E. coli* and *P. aeruginosa* sequences 1-4 were inactive with MIC >45.4 µg/mL. Sequences 5 and 7 showed MIC at 22.7 µg/mL against *E.coli* whereas; sequence 6 showed MIC at 2 fold higher concentration of 45.4 µg/mL. Against *P. aeruginosa* only sequence 7 showed growth inhibition with MIC at 22.7 µg/mL concentration.

Further to check if the designed sequences are growth inhibitory or bactericidal in nature, we performed killing kinetics at concentrations higher than MIC. Bactericidal activity is usually defined as ≥3 $\log_{10}$CFU reduction of initial inoculums. Sequences 5 and 6, at 2 × MIC showed bactericidal effect against MRSA upon 6h exposure (Fig. 5a). At 4 × MIC, sequence 5 showed rapid bactericidal effect upon 1h incubation whereas sequence 6 and 7 were able to reduce their initial inoculums by 3 $\log_{10}$CFU after 4h and 6h, respectively (Fig. 5b).

Fig. 5: Bactericidal kinetic of sequences 5-7 against MRSA at (a) 2 × MIC and (b) 4 × MIC. The symbols represent, control; (●), sequence 5 (■), sequence 6 (▲) and sequence 7 (◆).

On the whole, the sequences showed better potency against Gram-positive as compared to Gram-negative bacterial strains. It has been reported that the double bilayer structure of Gram-negative bacteria with outer lipopolysacharide coat impedes association with cationic antimicrobials (if the hydrophobic ends of the molecule are not well exposed) thereby decreasing effective concentration of antimicrobial agents that reach their target i.e. cytoplasmic membrane [42]. In another elegant work on polymer based supramolecular micelles it was shown that loosely packed self assemblies exposing both hydrophilic and hydrophobic ends showed broad spectrum of antibacterial activity against both Gram-positive as well as Gram-negative bacterial strains [17], whereas tight packed assemblies were specifically active against Gram-positive cells [43]. We extend the same to nano vesicles formed by sequences 5 and 6 designed in present work that showed a predominantly positively charged surface with less exposed hydrophobic interior leading to lesser potency on Gram-negative bacterial strains. Further, we observed that sequence 7 showed relatively broad spectrum activity with MIC<10 µg/mL against Gram-positive and MIC 22.7 µg/mL against tested Gram-negative bacterial strains which may further suggest role of relatively less tight packing in broad spectrum activity .

To establish cell selectivity of designed sequences their effect on hRBCs and A549 cells were studied under in vitro conditions. At 62.5 µg/mL, a concentration which was >20 times the MIC of sequences 5-7 against MRSA, non-significant hemolysis (<12%) was observed, whereas sequence 7 was completely non hemolytic at this concentration (Table 2). Results of the MTT assay on A549 cells

also showed >90% viability at 50 μg/mL for sequences 5 and 7 (Table 2).

Mechanism of interaction

Further to understand antibacterial mechanism we evaluated release of encapsulated calcein dye from artificial large unilamellar vesicles (LUVs) by monitoring changes in fluorescence on account of membrane destabilization caused by the designed sequences. The artificial lipid mixture used here (DOPC/DOPG, 7:3, w/w) provided a negative surface charge to the LUVs, thus roughly mimicking *S. aureus* cytoplasmic membranes. Sequences 5 and 7 showed burst release of encapsulated calcein dye where almost 78% leakage was observed at a concentration of 2.8 μg/mL. At highest tested concentration of 27.8 μg/mL almost 90% leakage occurred for both sequences 5 and 7 implicating excellent liposome lytic potential of these sequences. Sequence 6 at 2.8 μg/mL caused relatively less leakage with 55.4% content release however at 27.8 μg/mL, 78% leakage was observed for sequence 6 as well (Fig. 6a).

Fig. 6: (a) Dose response curve of encapsulated calcein leakage caused by designed sequences in (DOPC:DOPG, 7:3, w/w) LUVs and (b) membrane depolarization ability of sequences on intact MRSA using potential sensitive dye $DiSC_3(5)$. The symbols represent, sequence 5 (■), sequence 6 (▲) and sequence 7 (♦).

Bacterial cells maintain a relatively high negative trans-membrane potential as compared to eukaryotic cells. Next, to evaluate mechanism of action on intact cells, the ability of active sequences to alter membrane potential of MRSA cells was evaluated making use of potential sensitive dye $DiSC_3(5)$. An immediate and concentration dependent membrane depolarizing activity was observed for all three tested sequences 5-7. Interestingly, at highest tested concentration (12.5 μg/mL) sequence 7 was better able to alter membrane potential with 80.6% depolarization relative to 63.8 and 67.6% depolarization caused by sequences 5 and 6 respectively. It is interesting to note that nanovesicles formed by sequence 7 were most efficient at disruption of membrane potential as compared to more compactly packed nano vesicles formed by sequence 5 and 6 (Fig. 6b). Another important consideration here is the immediate effect of nanovesicles on intact *S. aureus* membrane potential as within two minutes of incubation the sequences were able to collapse membrane potential. The calcein leakage and potential depolarization experiments in tandem showed that the active sequences 5-7 were able to cause leakage of calcein dye from artificial membranes and destabilize membrane potential in intact cells thus indicating a membrane disruptive mode of action.

Further, to visualize morphological alterations caused by active sequences on *S. aureus* cells we incubated sequences 5, 6 and 7 with MRSA at concentrations higher than MIC (Fig. 7). Control MRSA cells exhibited bright smooth appearance with intact cell membrane (Fig. 7a). For sequence 5 treated cells; outer membrane rupturing with surface blebs as cellular protrusions was visible (Fig 7b). In sequence 6 treated cells deformed outer surface and flattened morphology were observed (Fig. 7c). On sequence 7 treatment also massive amount of mini cells protruding from existing cells were visible (Fig. 7d). Thus severe membrane destabilization ability of designed sequences was observed.

Fig. 7: Scanning electron microscopic images of MRSA (ATCC 33591) treated with designed active sequences at 10 × MIC for 30 min. The bar represents 200 nm.

Overall, our present work on amphiphilic template based sequences provides a platform to develop ultra short Trp-Arg and aromatic moiety based sequences that spontaneously self assemble in water. N-terminal capping with lipids and small organic moieties having inherent biological properties is well known for antibacterial peptidomimetics, a number of Arg and Trp rich sequences have also been reported [22, 23, 36], however our designed molecules are unique as along with a pharmacophore role the aromatic N-terminal tags serve to enhance hydrophobicity of Trp, Arg rich template which in turn promoted self assembly in designed sequences. Interestingly, the N-terminal tag could influence the nature of vesicles formed as well, where for sequence 5 and 6 we observed rigid nanovesicles with exposed hydrophilic surface only whereas for sequence 7, a dynamic assembly with both hydrophobic and hydrophilic portions exposed for interaction were observed. Of note, even dipeptides with aromatic amino acid residues have been shown to exhibit facile self assembly [44, 45], however to the best of our knowledge there are no reports of antibacterial activity for such dipeptide assemblies so far.

Further, the utility of Trp residues and aromatic tags in promoting aromatic stacking interactions was evident from CD and Trp fluorescence data. The increase in potency upon localized accumulation of cationic charge has previously been established to be a key factor for enhanced antibacterial potency for amphiphilic peptides and polymers [46]. Encouragingly potent antibacterial activity, cell penetration ability along with promising cell selectivity of similar short and cyclic Trp and Arg rich sequences has been reported recently [47, 48]. Our present work also established nano vesicle formation to be the underlying foundation for potency of the

designed sequences–(CAC data ensured presence and stability of nanovesicles at low concentrations). We hypothesize the lack of hydrophobicity upon initial interaction with Gram-negative bacterial cells to lead to poor activity of designed sequences 5 and 6 against *E. coli* and *P. aeruginosa*. This was further potentiated by relatively better activity of sequence 7 with slightly exposed hydrophobic surface (Trp residues and N-terminal tag) against Gram-negative bacterial cells. The elucidation of bactericidal mechanism showed a burst release of calcein dye from artificial membranes along with rapid membrane depolarization observed in live MRSA cells. Ultimately visualization of membrane morphology of *S. aureus* cells upon interaction with active sequences 5, 6 and 7 showed membrane damage, mini cell formation and leakage of intra cellular content to be major mode of action of these designed active sequences.

4. Conclusions

In conclusion, we present here novel cationic N-terminal tagged nano vesicles based on sequence amphilicity and aromatic stacking interactions. The N-terminal tag played a decisive role in nature of self assembly of vesicles formed by different sequences. Crucially, with a balance between positive charge and hydrophobicity sequences 5 and 6 form nanovesicles presenting a densely packed Arg cluster with positive surface zeta potential and an inner hydrophobic core comprising of aromatic N-terminal tagging and tryptophan residues that disrupts bacterial architecture upon interaction thus leading to potent activity against clinically relevant Gram-positive bacterial strains MRSA, MRSE, while maintaining cell selectivity. Sequence 7 with relatively dynamic nanovesicles was potent against both Gram-positive and Gram-negative bacterial strains, while at the same time maintaining a membrane disruptive mode of action and excellent cell selectivity. With small size making them cost effective, self assembling tendency and cell selectivity at present we are further exploring these nanovesicles as antibiotic delivery vehicles for systemic antibiotic therapy.

Acknowledgements

This work was financially supported by a Council of Scientific and Industrial Research (CSIR) network project BSC-0120. We thank Dr Souvik Maiti and Dr Kausik Chakraborty for useful discussions and instrumentation facility. Dr. Rita Kumar is acknowledged for microbial facility. We thank the Sophisticated Analytical Instrumentation Facility, All India Institute of Medical Sciences, New Delhi and Analytical Instrumental Research Facility at Jawahar Lal Nehru University, Delhi, India for providing us transmission electron microscopy and scanning electron microscopic facility respectively. The authors SJ and RPD are thankful to CSIR, New Delhi, India, for the award of senior research fellowship. The author SJ is also thankful to Dr. D.S. Kothari Postdoctoal fellowship University Grant Commission (UGC), India, for financial support. We thank Dr. Tandrika Chattopadhyay and Dr. Sarika Gupta, National Institute of Immunology for acquisition of AFM data.

References

1. M. McKenna, *Nature*, 2013, **499**, 394.
2. Antimicrobial resistance: global report on surveillance. 2014. World health organization. http://www.who.int/drugresistance/documents/surveillancereport/en/
3. L. L. Ling, T. Schneider, A. J. Peoples, A. L. Spoering, I. Engels, B. P. Conlon, A. Mueller, T. F. Schaberle, D. E. Hughes, S. Epstein, M. Jones, L. Lazarides, V. A. Steadman, D. R. Cohen, C. R. Felix, K. A. Fetterman, W. P. Millett, A. G. Nitti, A. M. Zullo, C. Chen and K. Lewis, *Nature*, 2015, **517**, 455.
4. M. Metz and D. M. Shlaes, *Antimicrob. Agents Chemother.*, 2014, **58**, 4253.
5. D. M. Easton, A. Nijnik, M. L. Mayer and R. E. Hancock, *Trends Biotechnol.*, 2009, **27**, 582.
6. M. Zasloff, *Nature,* 2002, **415**, 389.
7. C. D. Fjell, J. A. Hiss, R. E. Hancock and G. Schneider, *Nat. Rev. Drug Discov.*, 2011, **16**, 37.
8. D. Avarahami D and Y. Shai Y, *Biochemistry*, 2002, **41**, 2254.
9. R. M. Epand and R. F. Epand, *Mol. Biosyst*., 2009, **5**, 580.
10. K. A. Brogden, *Nat. Rev. Microbiol*., 2005, **3**, 238.
11. P. D. Rakowska, H. Jiang, S. Ray, A. Pyne, B. Lamarre, M. Carr, P. J. Judge, J. Ravi, U. I. Gerling, B. Koksch, G. J. Martyna, B. W. Hoogenboom, A. Watts, J. Crain, C. R. Grovenor and M. G. Ryadnov, *Proc. Natl. Acad. Sci. U S A*, 2013, **110**, 8918.
12. A. K. Marr, W. J. Gooderham and R. E. Hancock, *Curr Opin Pharmacol.*, 2006, **6**, 468.
13. B. Mensa, G. L. Howell, R. Scott and W. F. DeGrado, *Antimicrob. Agents Chemother.*, 2014, **58**, 5136.
14. N. Ooi, K. Miller, J. Hobbs, W. Rhys-Williams, W. Love and I. Chopra, *J. Antimicrob. Chemother.*, 2009, **64**, 735.
15. C. Chen, F. Pan, S. Zhang, J. Hu, M. Cao, J. Wang, H. Xu, X. Zhao and J. R. Lu, *Biomacromolecules*, 2010, **11**, 402.
16. D. Xu, L. Jiang, A. Singh, D. Dustin, M. Yang, L. Liu, R. Lund, T. J. Sellati and H. Dong, *Chem. Commun.*, 2015, **51**, 1289.
17. Y. Qiao, C. Yang, D. J. Coady, Z. Y. Ong, J. L. Hedrick and Y. Y. Yang. *Biomaterials*, 2012, **33**, 1146.
18. A. P. McCloskey, B. F. Gilmore and G. Laverty, *Pathogens*, 2014, **3**, 791.
19. J Ravi, A. Bella, A. J. Correia, B. Lamarre and M. G. Ryadnov, *Phys. Chem. Chem. Phys.,* 2015, **17**, 15608.
20. D. I. Chan, E. J. Prenner and H. J. Vogel, *Biochim Biophys Acta,* 2006, **1758**, 1184.
21. L. Zhigang, A. Brady, A. Young, B. Rasimick, K. Chen, C. Zhou and N. R. Kallenbach, *Antimicrob. Agents Chemother.*, 2007, **51**, 597.
22. B. Deslouches, J. D. Steckbeck, J. K. Craigo, Y. Doi, T. A. Mietzner and R. C. Montelaro, *Antimicrob. Agents Chemother.*, 2013, **57**, 2511.
23. R. Saravanan, X. Li, K. Lim, H. Mohanram, L. Peng, B. Mishra, A. Basu, J. M. Lee, S. Bhattacharjya and S. S. Leong, *Biotechnol. Bioeng.,* 2014, **111**, 37.
24. S. Joshi, R. P. Dewangan, S. Yadav, D. S. Rawat and S. Pasha, *Org Biomol Chem.* 2012, **10**, 8326.
25. S. Yadav, S. Joshi, M. A. Q. Pasha and S. Pasha, *Med. Chem. Commun.*, 2013, **4**, 874.
26. R. P. Dewangan, S. Joshi, S. Kumari, H. Gautam, M. S. Yar and S. Pasha. *Antimicrob. Agents Chemother.*, 2014, **58**, 5435.
27. R. B. Merrifield, *Science*, 1986, **232**, 341.
28. M. M. Konai, C. Ghosh, V. Yarlagadda, S. Samaddar and J. Haldar, *J. Med. Chem.*, 2014, **57**, 9409.
29. W. L. Zhu, Y. M. Song, Y. Park, K. H. Park, S. T. Yang, J. Kim, S. Park, K. S. Hahm and S. Y. Shin, *Biochim. Biophys. Acta*, 2007, **1768**, 1506.
30. S. Joshi, G. S. Bisht, D. S. Rawat, A. Kumar, R. Kumar, S. Maiti and S. Pasha., *Biochim Biophys Acta.*, 2010, **1798**, 1864.
31. M. A. Wikler, D. E. Low, F. R. Cockerill, D. J. Sheehan, W. A. Craig, F. C. Tenover and M. N. Dudley, Methods for dilution antimicrobial susceptibility tests for bacteria that grow aerobically: approved standard-seventh edition, CLSI (formerly NCCLS) (2006) M7-A7.
32. S. T. Yang, J. Y. Lee, H. J. Kim, Y. J. Eu, S. Y. Shin, K. S. Hahm and J. I. Kim, *FEBS J*, 2006, **273**, 4040.
33. L. Schmidtchen, G. Ringstad, H. Kasetty, M. W. Mizuno, M. Rutland and M. Malmsten, *Biochim. Biophys. Acta*, 2011, **1808**, 1081.
34. P. N. Domadia, A. Bhunia, A. Ramamoorthy and S. Bhattacharjya, *J. Am. Chem. Soc.*, 2010, **132**, 18417.
35. T. Hansen, T. Alst, M. Havelkova and M. B. Strom, *J. Med. Chem.*, 2010, **53**, 595.
36. R. O. Jahnsen, A. Sandberg-Schaal, N. Frimodt-Moller, H. M. Nielsen and H. Franzyk, *Eur. J. Pharm. Biopharm.* 2015, doi: 10.1016/j.ejpb.2015.01.013.
37. E. Neil, G. Marsh, B. C. Buera and A. Ramamoorthy, *Mol. BioSyst.*, 2009, **5**, 1143.
38. S. Z. Tian, X. Pu, G. Luo, L. X. Zhao, L. H. Xu, W. J. Li and Y. Luo, *J. Agric. Food Chem.* 2013, **61**, 3006.
39. R. P. Lamers, J. F. Cavallari and L. L. Burrows, *PLoS One*, 2013, **8**, e60666.
40. M. Nichols, M. Kuljanin, M. Nategholeslam, T. Hoang, S. Vafaei, B. Tomberli, C. G. Gray, L. DeBruin and M. Jelokhani-Niaraki, *J. Phys. Chem. B*, 2013, **117**, 14697.
41. S. Singh, P. Papareddy, M. Kalle, A. Schmidtchen and M. Malmsten, *RSC Adv.*, 2014, **4**, 37582.
42. K. Lienkamp, K. N. Kumar, A. Som, K. Nusslein and G. N. Tew, *Chemistry*, 2009, **15**, 11710.
43. F. Nederberg, Y. Zhang, J. P. K. Tan, K. Xu, H. Wang, C. Yang, S. Gao, X. D. Guo, K. Fukushima, L. Li, J. L. Hedrick and Y. Y. Yang, *Nat. Chem.*, 2011, **3**, 409.
44. M. Reches and E. Gazit, *Phys Biol.*, 2006, **2**, S10-9.
45. A. Mishra, J. J. Panda, A. Basu and V. S. Chauhan, *Langmuir*, 2008, **24**, 4571.
46. L. Liu, K. Xu, H. Wang, P. K. Tan, W. Fan, S. S. Venkatraman, L. Li and Y.Y. Yang, *Nat. Nanotech.*, 2009, **4**, 457.
47. D. Oh, J. Sun, S. A. Nasrolahi, K. L. LaPlante, D. C. Rowley and K. Parang, *Mol. Pharm.,* 2014, **11**, 3528.
48. D. Mandal, S. A. Nasrolahi and K. Parang, *Angew Chem Int Ed Engl.*, 2011, **50**, 9633.

Table 1: Sequence, composition, percentage hydrophobicity, size/PDI, zeta potential and CAC of designed sequences

Sequence	Composition	% hydrophobicity[a]	Size (nm)/PDI[b]	Zeta potential (mV)	CAC[c] (μg/mL)
1	RRRR-$CONH_2$	11.2	-	-	-
2	WRRRR-$CONH_2$	15.1	-	-	-
3	WWRRRR-$CONH_2$	41.1	-	-	-
4	WWWRRRR-$CONH_2$	50.3	-	-	-
5	X_1-WWWRRRR-$CONH_2$	64.8	169.5/0.081	47.9	0.2
6	X_2-WWWRRRR-$CONH_2$	74.5	140.7/0.165	45.9	3.0
7	X_3-WWWRRRR-$CONH_2$	62.8	184.8/0.376	40.7	3.9

[a]percentage of acetonitrile at RP-HPLC elution, [b]polydispersity index, [c]critical aggregation concentration was determined in MHB II growth media using light scattering, X_1:2-Fluoro-3-(trifluoromethyl)benzoic acid, X_2: p-Terphenly-4-carboxylic acid, X_3: 2-Methyl-1-naphthoic acid

Table 2: Antibacterial activity of designed sequences against a panel of bacterial strains

	MIC (μg/mL)								Toxicity	
	Gram-positive bacteria						Gram-negative bacteria			
	S. aureus (ATCC 29213)	*E. faecalis* (ATCC 7080)	*S. epidermidis* (ATCC 12228)	*S. aureus*[a] (ATCC BAA-44)	MRSE (ATCC 51625)	MRSA (ATCC 33591)	*E.coli* (ATCC 11775)	*P. aeruginosa* (ATCC 25668)	% H[b]	% viability[c]
1	>45.4	>45.4	ND	ND	ND	>45.4	>45.4	>45.4	0	ND
2	>45.4	>45.4	ND	ND	ND	>45.4	>45.4	>45.4	0	ND
3	>45.4	>45.4	ND	ND	ND	>45.4	>45.4	>45.4	0	ND
4	45.4	>45.4	ND	ND	ND	>45.4	>45.4	>45.4	0	ND
5	1.4	5.6	0.7	1.4	0.7	2.8	22.7	45.4	8	90.4
6	2.8	11.3	1.4	2.8	1.4	2.8	45.4	>45.4	10	ND
7	1.4	5.6	0.7	1.4	0.7	1.4	22.7	22.7	0	99.8
PXB	16	32	22.7	45.4	11.5	32	0.7	0.7	ND	ND

[a]Ciprofloxacin resistant strain, [b]percentage hemolysis at 62.5 μg/mL, [c]percentage viability at 50 μg/mL, PXB: polymyxin B, ND: not determined

Journal Name

ARTICLE

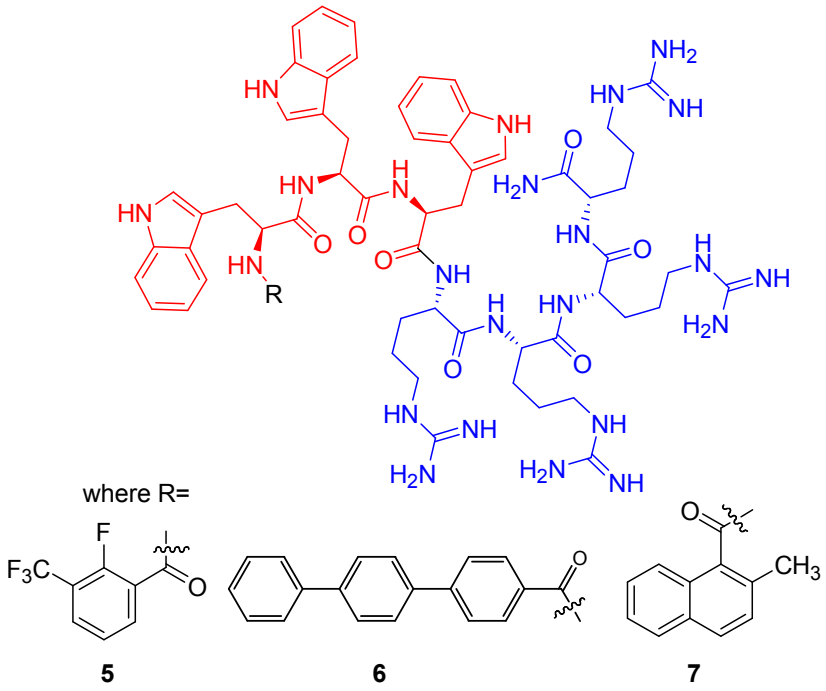

Fig. 1: Structural representation of designed template and different N-terminal tags. The hydrophilic residues are coloured blue and hydrophobic residues are coloured red.

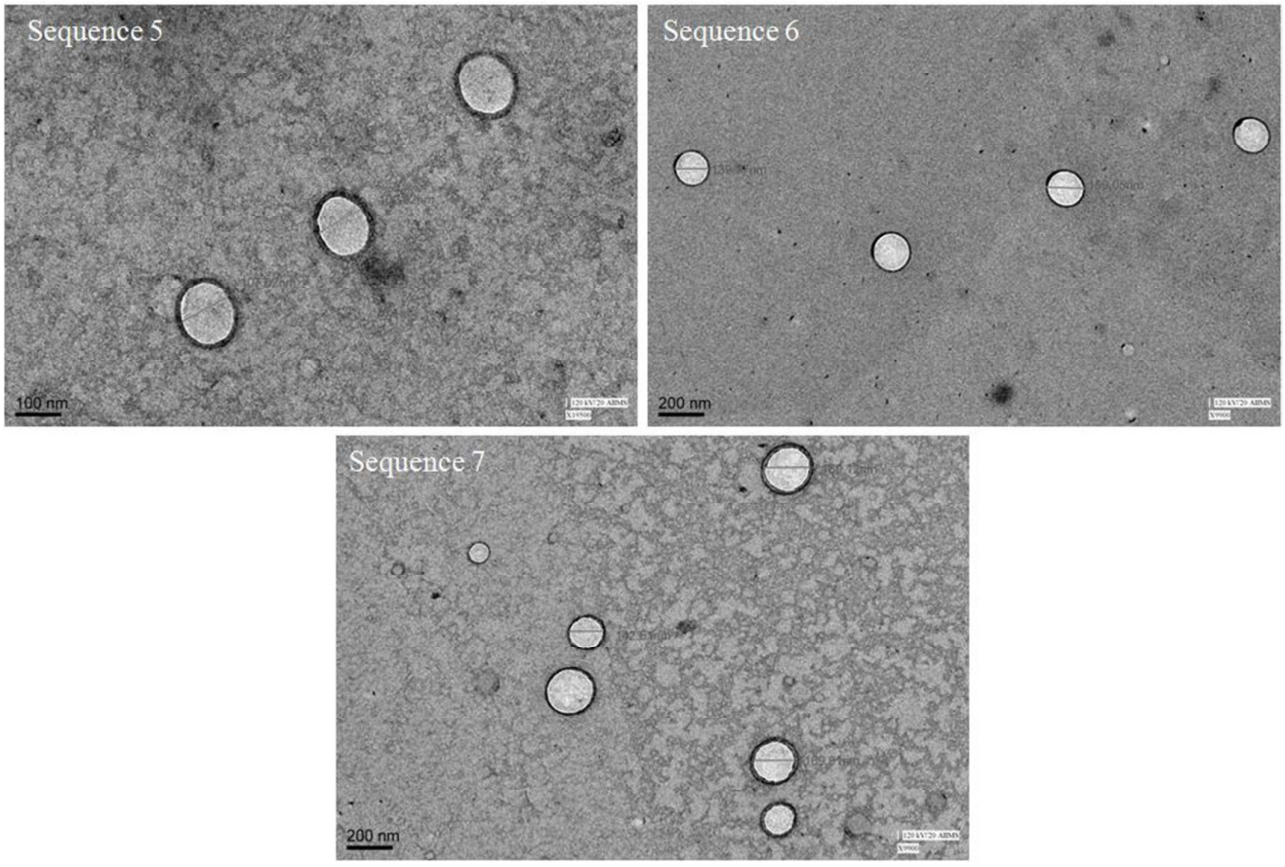

Fig. 2: Transmission electron microscopic images of sequences 5-7 in water.

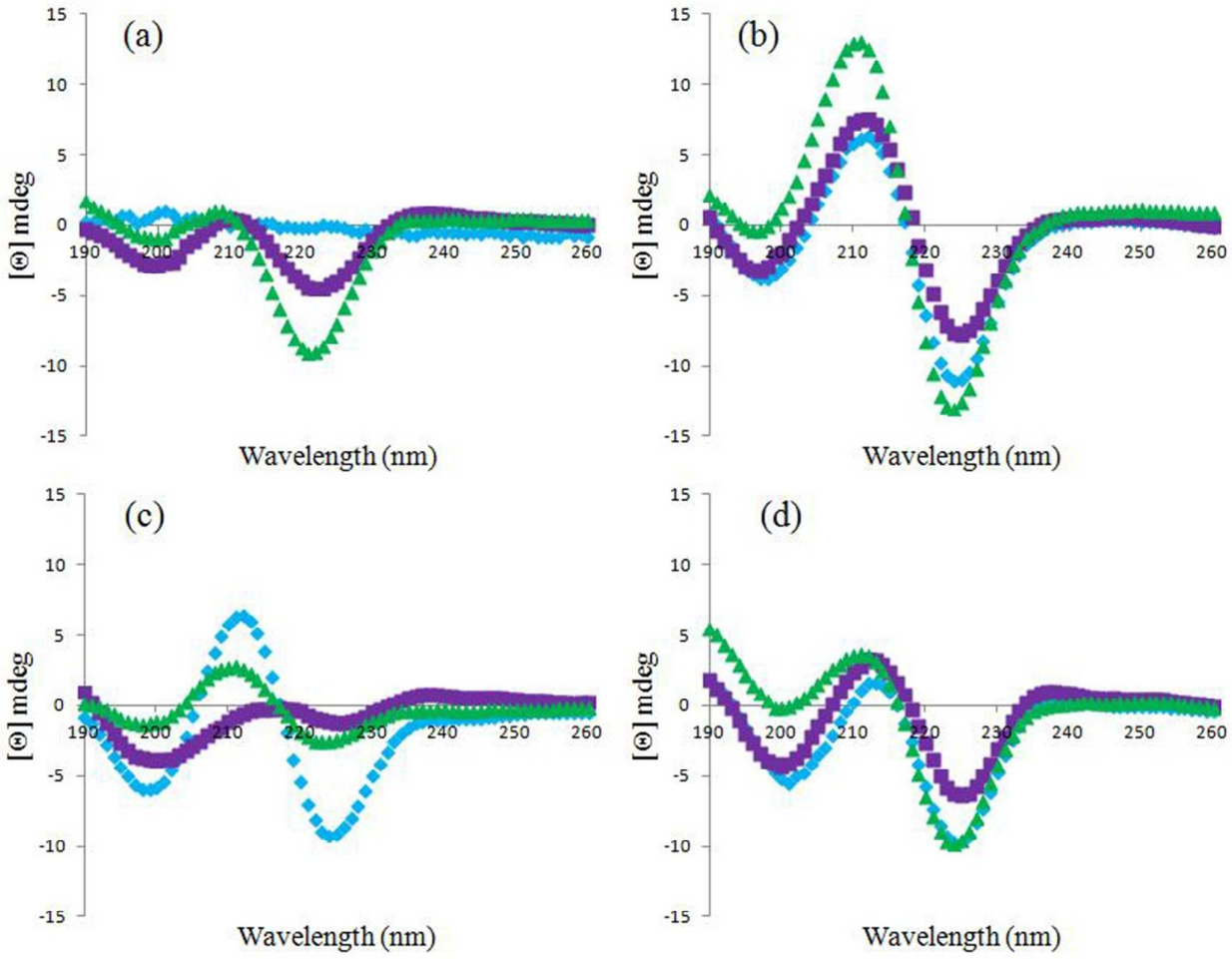

Fig. 3: CD spectra of designed sequences in different environments; water (◆), phosphate buffer (▪) and 50% TFE (v/v) (▲). In (a) Sequence 4, (b) sequence 5, (c) sequence 6 and (d) sequence 7. The spectrum was acquired at a sample concentration of 20 µg/mL.

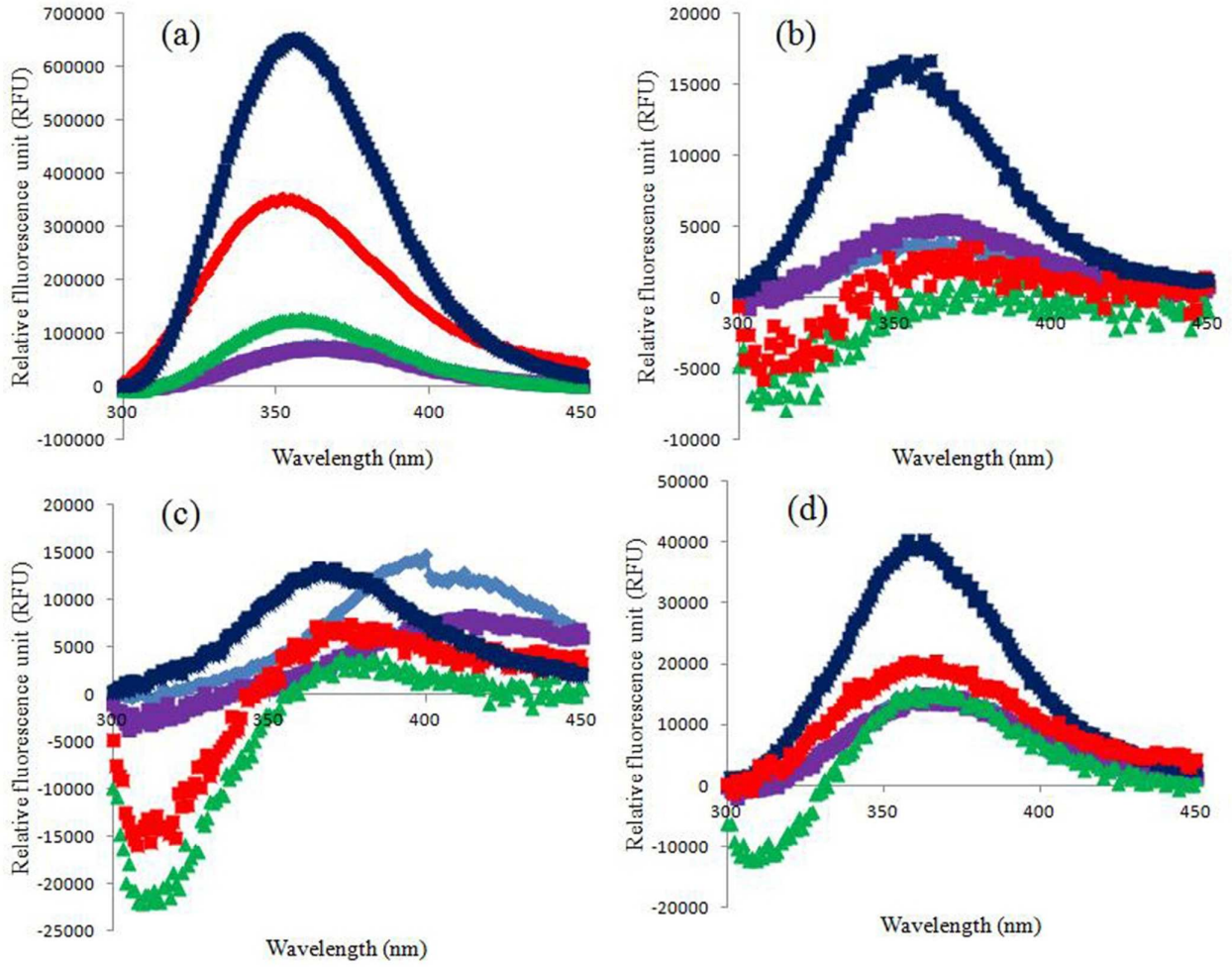

Fig. 4: Trptophan fluorescence spectra of designed sequences in different environments; water (◆), 10 mM Tris buffer (▬) DOPC (▲) DOPC/DOPG (■) and DMSO (■). In (a) Sequence 4, (b) sequence 5, (c) sequence 6 and (d) sequence 7. The spectrum was acquired at a sample concentration of 5 µg/mL.

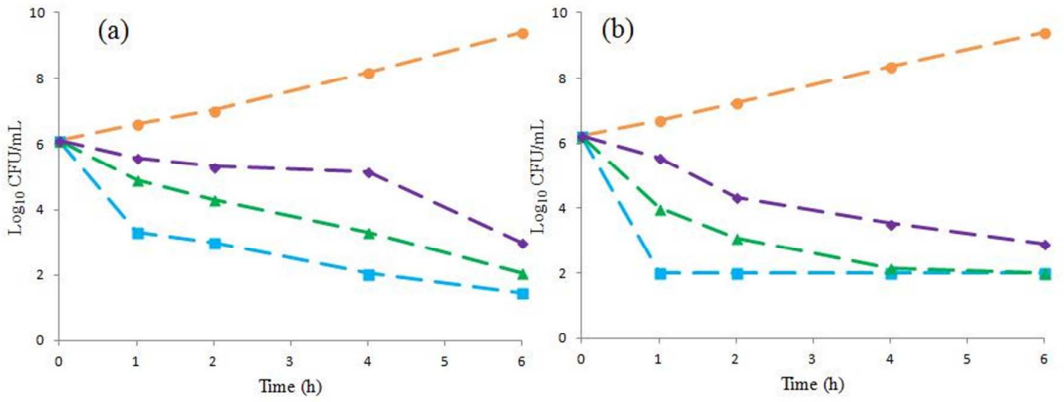

Fig. 5: Bactericidal kinetic of sequences 5-7 against MRSA at (a) 2 × MIC and (b) 4 × MIC. The symbols represent, control; (●), sequence 5 (■), sequence 6 (▲) and sequence 7 (♦).

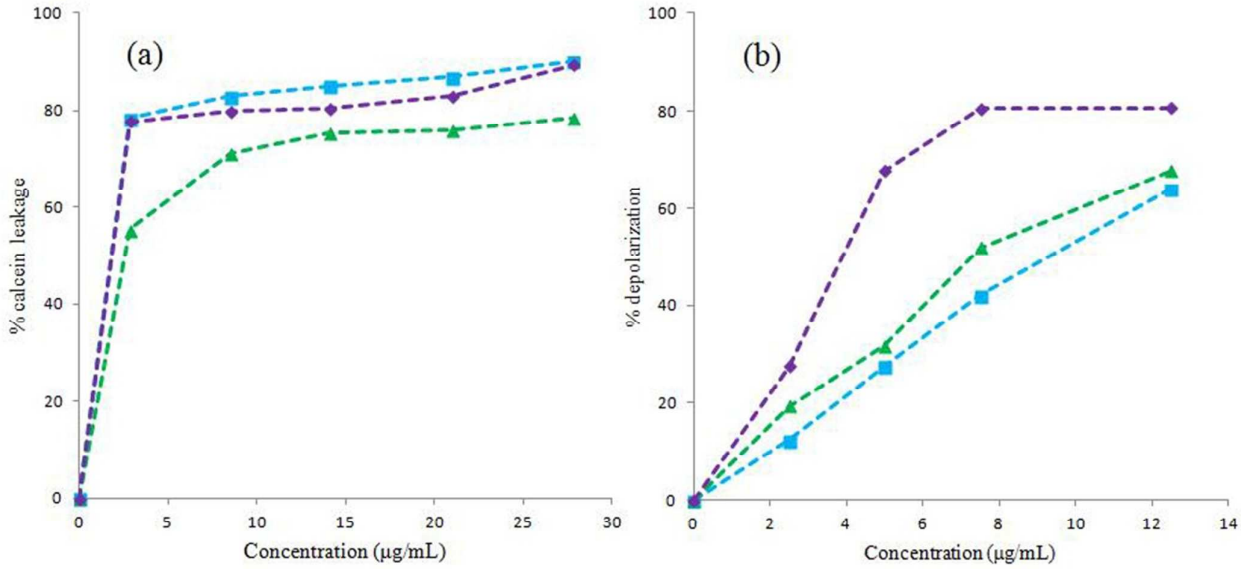

Fig. 6: (a) Dose response curve of encapsulated calcein leakage caused by designed sequences in (DOPC:DOPG, 7:3, w/w) LUVs and (b) membrane depolarization ability of sequences on intact MRSA using potential sensitive dye $DiSC_3(5)$. The symbols represent, sequence 5 (■), sequence 6 (▲) and sequence 7 (♦).

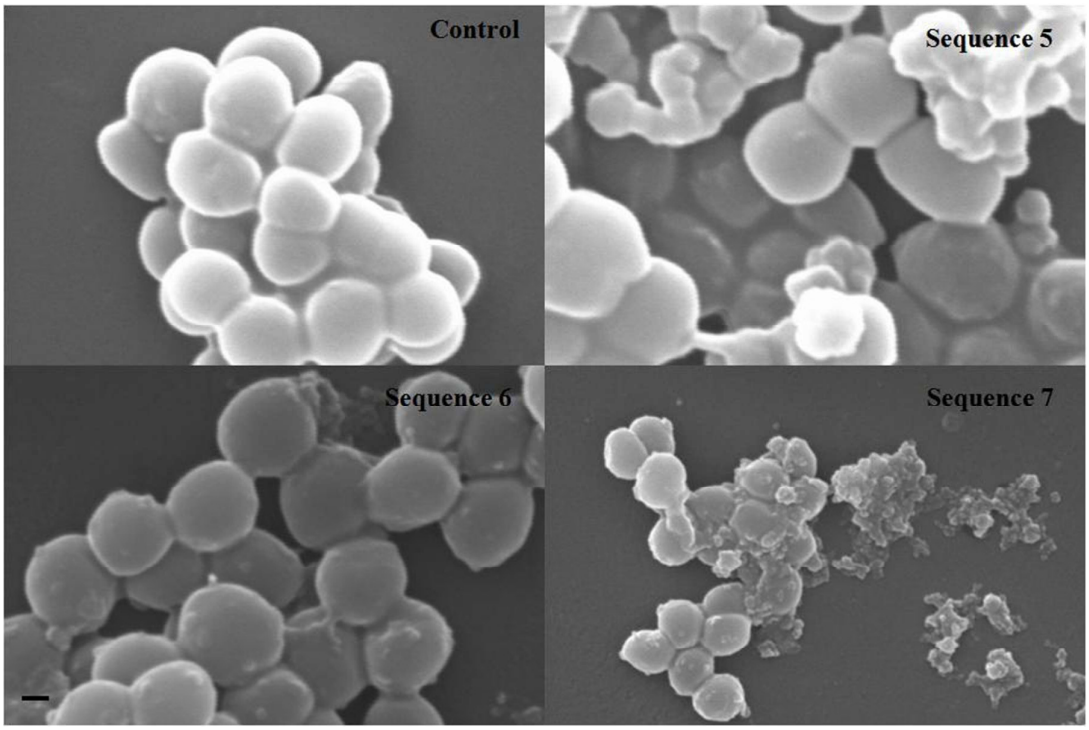

Fig. 7: Scanning electron microscopic images of MRSA (ATCC 33591) treated with designed active sequences at 10 × MIC for 30 min. The bar represents 200 nm.

N-Terminal Aromatic Tag Induced Self Assembly of Tryptophan-Arginine Rich Ultra Short Sequences and Their Potent Antibacterial Activity

Seema Joshi,[a, b] Rikeshwer P. Dewangan,[a, c] Mohammad S. Yar[c], Diwan S. Rawat[d] and Santosh Pasha[a, *]

[a]CSIR- Institute of Genomics and Integrative Biology, Mall Road, Delhi, India

[b]Current affiliation: School of Environmental Sciences, Jawaharlal Nehru University, Delhi, India

[c]Department of Pharmaceutical Chemistry, Faculty of Pharmacy, Jamia Hamdard, New Delhi, India

[d]Department of Chemistry, University of Delhi, Delhi, India

[*]Email: spasha@igib.res.in

Table of contents

Novel, ultra short, N-terminal modified tryptophan-arginine rich sequence undergoes facile self assembly in water and exhibit excellent anti-MRSA activity